

Radiometric Calibration of Cartosat-2 panchromatic sensor using artificial targets

a prelude to Cartosat-2C



Scientific Report

CAL-VAL Team

May- 2016



**Calibration and Validation Division
Earth, Ocean, Atmosphere, Planetary Sciences & Applications Area
Space Applications Centre (ISRO)
Ahmedabad - 380 015**

CAL-VAL Team

1. Space Applications Centre (SAC-ISRO), Ahmedabad

Mrs. Shweta Sharma- Principal Investigator

Mr. R.P. Prajapati- Co-Principal Investigator

Dr. A K Mathur- Coordinator

Field-data collection support provided by:

Mr. Mihir Rambhia, JRF, M.G. Science Institute

Mr. Vikram S. Kanhaiyalal, Apprentice, SAC-ISRO

Mr. Viramgami Mayur, Apprentice, SAC-ISRO

DOCUMENT CONTROL SHEET

1. Report No.	SAC/EPESA/CVD/CAL-VAL/TR/01/05/2016
2. Publication date	May 2016
3. Title and subtitle	Radiometric Calibration of Cartosat-2 panchromatic sensor using artificial targets: <i>prelude to Cartosat-2C</i>
4. Type of report	Scientific
5. Number of pages	5 + 21
6. Number of references	5
7. Authors	CAL-VAL Team
8. Originating unit	CVD- EPESA
9. Abstract	<p>In this study, the calibration constants for Cartosat-2 sensor were estimated using the artificial targets (black cloth and white cloth) deployed prior to Cartosat-2 pass and ground and atmospheric parameters' measurements carried out synchronous to the satellite pass. Two independent approaches were used for the estimation. One being the vicarious calibration, which is popularly used world-wide and other being physics based simple analytical approach. The calibration activity indicates the change in the calibration constant for Cartosat-2 sensor. Both the vicarious and analytical approach show matching results in the estimated mean value of multiplicative factors by vicarious and analytical approach. This exercise will help in the radiometric calibration of upcoming high resolution optical sensor viz. Cartosat-2C panchromatic and multispectral sensors using one date ground measurements only.</p>
10. Key words	Radiometric calibration, Cartosat-2, artificial targets, vicarious calibration
11. Security classification	Unrestricted
12. Distribution statement	General

TABLE OF CONTENTS

	Page No.
Table of Contents	4
Summary	5
1. Introduction	6
2. Objectives	8
3. Study Area and Data used	8
3.1 Study Area	8
3.2 Data and material used	9
3.3 Sampling strategy	9
4. Methodology used	10
4.1 Estimation of calibration constant using vicarious calibration approach	10
4.2 Estimation of calibration constant using simple analytical approach	15
5. Results and Discussions	17
5.1 Results using vicarious calibration approach	19
5.2 Results using simple analytical approach	23
6. Conclusions	24
Acknowledgements	25
References	26

SUMMARY

This report brings out the results of independent calibration exercise carried out by the calibration and validation team for Cartosat-2 panchromatic sensor. The calibration constants were estimated by deploying artificial targets (black cloth and white cloth) prior to the Cartosat-2 pass and surface reflectance data and atmospheric parameters were collected synchronous to the pass. The calibration constants were estimated using two independent approaches, one being the vicarious calibration, which is used world-wide and other being physics based simple analytical approach. The multiplicative factor and additive factors were estimated using one date data only contrary to the method where large number of satellite image data is required for the estimation of calibration constant.

This calibration activity indicates the change in the calibration constant for Cartosat-2 panchromatic sensor. The value of the multiplicative factor estimated using vicarious approach was found to be 0.475 ± 0.013 with additive factor being -46 ± 2.4 . The results obtained using the vicarious and analytical approach show excellent matching between the estimated mean value of multiplicative factors by vicarious and analytical approach. Although, more number of data is required for the refinement of the analytical model. This exercise will help in the radiometric calibration of upcoming high resolution optical sensor viz. Cartosat-2C panchromatic and multispectral sensors using one date ground measurements only.

1. Introduction

Various applications require accurate, well calibrated and characterized measurements. Numerical weather prediction and climate change detection studies critically depend on accurate, reliable and consistent satellite radiance data. In order to extract accurate and reliable quantitative information from digitally remotely sensed data, it is necessary and essential to properly calibrate the sensor and validate the associated data products. Calibration is the process of quantitatively defining the satellite instrument response to known controlled signal inputs. The inputs can range from a well-defined, standard lamp source in the laboratory and on-orbit satellite as well as field measurements over a large (relative to pixel size) homogeneous land/water area. A sensor calibration coefficient relates a digital number (DN) observed in an image pixel to its radiance, which is a physical quantity characterizing the radiative property of an earth surface feature represented by the pixel. Before satellite launch, sensor calibration coefficients are derived in the laboratory by measuring sensor-detector response to illumination from a well-defined, standard source of light, traceable to well-known standards such as NIST (National Institute of Standards). The output from the detectors within a sensor in response to a known, well characterized source of radiance is quantized to a discrete number of quantized gray levels (DN), where the radiance is the input and DN is the output. The methods and protocols involved in prelaunch, laboratory measurements of calibration coefficients have been comprehensively reviewed in a CEOS report (Datla et al, 2011). However, the satellite data available to the users is in the form of quantized DN values which can be converted to radiance using the general calibration relation:

$$L = a*DN + b \quad (1)$$

where, L is radiance in units of W/m²/sr/μm, DN is the quantization value expressed as an integer in a satellite image, and 'a' and 'b' are coefficients, in units of radiance per unit count (DN). The coefficients 'a' and 'b' (also called gain and offset respectively) are different for

each wavelength for different satellite sensors and are usually supplied in the satellite header file. The quantized DN values can range between 0 and 2^n , where n is the number of bits used for digitally encoding the data. For example, for $n=8$, the maximum value is 255 and for $n=10$, the maximum value is 1023, with zero as the starting value. Equation (1) implies that the calibration relation is usually developed over the linear response region of a detector/sensor. The task of vicarious calibration is to estimate the 'a' and 'b' coefficients in eqn. (1), post-launch, using field measurements over selected homogeneous test sites.

There are many methods of vicarious calibration, viz., absolute vicarious calibration, relative calibration, lunar calibration etc. that can be used to monitor possible variations in sensor calibration coefficients. Vicarious calibration refers to the process of determining a sensor calibration coefficient using field measured surface radiance/reflectance, in-situ atmospheric measurements concurrent with satellite pass and sensor observed DN values of the same surface, at the time of satellite pass. An obvious and critical requirement for vicarious calibration is the selection of a suitable spatial and temporal stable (ideally invariant) site and a set of well calibrated field instruments for measuring surface reflectance and atmospheric variables conforming to primary SI standards traceable to NIST.

In order to estimate the calibration coefficients (a and b in equation 1) for in-flight radiometric calibration of satellite optical sensors, a large number of field measured data (sub-satellite ground based measurements of atmospheric parameters and surface reflectance data) synchronous to satellite pass is required. This requires more number of field campaigns, resulting in much greater human efforts which in turn makes it a tedious and time taking process. Therefore, there is a need to evolve a methodology which will help in reducing the time and effort and produce quick results. In the present study, it is proposed to estimate the calibration coefficients with only one date data by utilizing the artificial targets for high

resolution optical sensors. For the study, a mathematical equation has been formulated based on the literature.

2. Objectives

The detailed objectives of the proposed study are to estimate the calibration coefficients of high resolution data Cartosat-2 with one date field measurements utilizing the artificial targets (black and white cloth).

3. Study Area and Data Used

3.1 Study Area: SAC-Bopal cal-val site in Ahmedabad was used as a study site for the study. This site has been developed for vicarious calibration of high resolution optical as well as SAR sensors. It has been artificially created by SAC adjacent to Bopal campus. The site consists of a very uniform levelled bare land (yellow in color) of 115m x 115m with very clear brick boundary constructed on all four sides and 4m x 4m concrete white squares on the four corners of the site. Figure 1 shows its location (marked by yellow circle) on the google earth image.

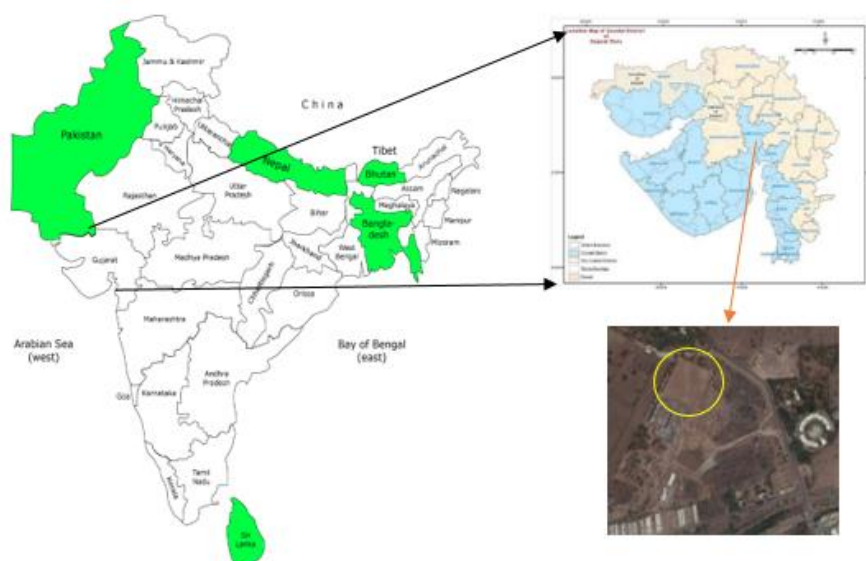


Figure 1: Calibration site near SAC, Bopal Campus [courtesy: Google Earth]

3.2 Data and material used

High resolution Cartosat-2 data (1m spatial resolution) of 3rd May 2016 was used for the study. For artificial targets, we used black cloth of 5m * 5m and white cloth of 6m * 6m (Figure 2).



Figure 2: Artificial targets deployed at calibration site near SAC, Bopal Campus

3.3 Sampling strategy

A sampling grid plan of 3m * 3m pixels was adopted for all the three targets (black cloth, soil and white cloth) at Bopal site for characterizing surface reflectance and associated atmospheric measurements. This choice is dictated partly by practical constraints, viz., the measurements have to be completed preferably within ± 30 minutes of satellite pass and to avoid boundary pixels. Measurements were confined to 3*3 pixels i.e. 3m * 3m in order to avoid path adjacency effect for all the three targets (high reflectivity, low reflectivity and soil target). For satellites under consideration here i.e. for Cartosat-2, the spatial resolution is 1m which corresponds to approximately 3m * 3m area on the ground (Figure 3).



**Figure 3: Sampling plan for the measurements
(measurements were confined to 3m * 3m pixels)**

4. METHODOLOGY USED

The estimation of calibration constants was done using two approaches: (i) by using vicarious calibration approach and radiative transfer model 6S and (ii) by using simple analytical approach. Both the approaches are described as follows:

4.1 Estimation of calibration constant using Vicarious calibration approach

Before launch, the pre-launch calibration procedure in the laboratory results in a set of calibration coefficients (counts per unit radiance) for each spectral band, mapping digital numbers to radiances. In the post-launch phase, average radiance measurements over a test site are input to an atmospheric model to estimate at-sensor radiance. A relation between the average DN and radiance at satellite level yields a set of wavelength dependent calibration coefficients which are then compared with pre-launch calibration coefficients (Dingirard and Slater, 1999). If radiances/reflectances are given in the digital products, then the computed at-

sensor radiance/reflectance will be compared directly with observed satellite radiance/reflectance. This is the scheme for absolute calibration of sensors.

Vicarious calibration method was used for estimating the calibration constant. It is, in principle, a comparison of estimated TOA radiance with satellite measured radiance over the same ground area at the same time. Alternatively, the quantized DN sensor values are converted to radiance using pre-launch calibration coefficients, and an atmospheric correction code is applied to retrieve surface reflectance, which is then compared with field measured reflectance. In this study, the 6S code (Vermote et al. 2006) is used in forward mode to estimate TOA radiance for a measured field reflectance and atmospheric parameters. In the inverse mode, the surface reflectance is retrieved from TOA radiance or reflectance with the same atmospheric parameters. The simulated TOA radiance computed in the forward mode is compared with satellite measured radiance to estimate the radiance ratio. The comparison is done by comparing mean radiance with 1σ error limits. Surface reflectance of the three targets (black cloth, white cloth and soil) is measured using ASD spectro-radiometer synchronous to Cartosat-2 pass and atmospheric measurements were done using Microtops-II sunphotometer and ozonometer. The details of data analysis are as follows:

Step 1: Field-measured spectral reflectance (350–2500 nm) from the site was first exported to Excel format using ViewSpecpro software for all the three targets.

Step 2: Reflectance data (averaged over 3*3 pixels for each target at 1 nm interval) relevant to Cartosat-2 panchromatic band was extracted over the bandwidth corresponding to 5% cut-off of sensor's RSR. In this study, the surface reflected flux recorded by the sensor over 5% cut-off bandwidth is used to compute TOA radiance.

Step 3: Both the SRF (spectral response function) and reflectance data were re-sampled to 2.5 nm intervals using a spline interpolation method using MATLAB code. This was done since the 6S code requires that both SRF and surface reflectance data are input at 2.5 nm intervals.

Step 4: The 6S code was used to compute TOA radiance. The inputs are sun-sensor geometry (sun and view zenith and azimuth angles), atmosphere model, aerosol model, AOD, levels of ozone and water vapour, and ground reflectance.

Step 5: Using the TOA radiance estimated for all the three targets and corresponding average DN value observed from Cartosat-2 image data, calibration coefficients (gain and offset) was estimated for panchromatic band.

In the 6S code, when measured values of water vapour and ozone are given as input, the code assumes the US 62 standard atmosphere profile for computations (Vermote et al. 2006). The US 62 atmosphere profile gives pressure, temperature, water vapour, and ozone concentrations as a function of height (up to 100 km), at discrete intervals of 34 layers. The continental aerosol model consists of a mixture of dust-like, water-soluble, and soot components in fixed proportions. For a given aerosol model, the code computes the extinction coefficient, single scattering albedo, asymmetry parameter, and phase function using Mie theory. In forward mode, the 6S code computes TOA reflectance and radiance for given surface reflectance, while in the inverse mode the code computes atmosphere-corrected surface reflectance for the same atmospheric parameters as in the forward model, for a given TOA at-satellite radiance input. The 6S code is a point based code (and not an image based code), i.e. the inputs are given for a single pixel.

The vicarious calibration procedure attempts to provide a known, measured at-sensor TOA radiance (by making surface reflectance and atmospheric measurements) which is compared with satellite measured radiance of the same surface at the same time. Since the experimental

site is characterized by its mean and standard error, for an ideal sensor, the radiance ratio should be equal to one, within 1 standard error limits. It follows that any deviation from unity (within one standard error) indicates a possible sensor calibration problem.

Since the 6S code estimates atmospherically corrected surface reflectance in the inverse mode, the same dataset can also be used for its validation. This is done by studying the correlation between measured and estimated surface reflectance.

Uncertainty Analysis

For uncertainty analysis, the approach used by V.N. Sridhar *et al.* (2013) was used in this study. TOA-estimated radiance is a function of many variables (i.e. solar and viewing geometry, field spectral reflectance in different wavelength bands, atmospheric variables, and sensor spectral response functions). The functional dependence of TOA radiance on these variables is complex and it is often not possible to express it in a closed, analytical form. In such cases, a functional approach is adopted, where the value of the dependent variable for specific values of the independent variable (e.g. mean $\pm 1\sigma$) is computed, and taken as a measure of uncertainty in the dependent variable. Field measurements were carried out at different locations within a study site for a given date, and the mean and standard deviation were computed for that site. Here, the standard deviation is taken as a measure of uncertainty for the site for the relevant variables, while the mean value is assumed to be the best estimate of a given variable.

The sources of uncertainty considered in this study are (i) spatial variability of field reflectance, (ii) variability of AOT, (iii) variability of water vapour, (iv) variability of ozone, and (v) anisotropy of surface reflectance. The solar and viewing geometry, as well as spectral response functions, are treated as fixed values for a given site and date, while the measured standard deviations in the variables are used to estimate uncertainties in TOA mean radiance. The effect of each of these uncertainties on TOA radiance was evaluated here based on a functional

approach (Hughes and Hase 2010). In this approach, TOA radiances corresponding to the (mean + 1 σ) and the (mean - 1 σ) are computed to estimate uncertainty in TOA radiance for that variable. Specifically, TOA radiance is modelled as:

$$R^{\text{TOA}} = f(\rho^{\text{surf}}, \text{AOT}, \text{WV}, \text{O}_3, \rho^{\text{anis}}). \quad (7)$$

where R^{TOA} is TOA radiance (W cm⁻² sr⁻¹ μm^{-1}), ρ_{surf} is surface Lambertian reflectance (dimensionless), AOT is aerosol optical thickness (dimensionless), WV is water vapour level (g cm⁻²), O₃ is ozone level (in cm-atmospheres), and ρ_{anis} is surface reflectance anisotropy (dimensionless). The functional dependence of R^{TOA} on these variables is denoted by f, which cannot be expressed in a closed analytical form. The best estimate of R^{TOA}, R^{TOA}_m, is given by:

$$R_m^{\text{TOA}} = \rho_m^{\text{surf}}, \text{AOT}_m, \text{WV}_m, \text{O}_{3m}. \quad (8)$$

where the subscript m refers to mean values of the variables. The mean values of the above variables are input to the 6S code to estimate mean values of TOA radiance in different bands. The uncertainty in R^{TOA}_m is calculated by perturbing each of the four independent variables (ρ_m^{surf} , AOT_m, WV_m, and O_{3m}) by $\pm 1\sigma$ from their mean values for the four variables.

$$\Delta R_{m,i}^{\text{TOA}} = (R_{m+\sigma,i}^{\text{TOA}} - R_m^{\text{TOA}}), i = 1 \dots 4, \quad (9)$$

where $\Delta R_{m,i}^{\text{TOA}}$ is the uncertainty in TOA radiance due to uncertainty in surface reflectance and i = 2, 3, 4 represents the corresponding uncertainty due to AOT, WV, and O₃, respectively.

The total uncertainty in R^{TOA}_m, ΔR_m^{TOA} , is then the quadrature sum of each uncertainty:

$$\Delta R_m^{\text{TOA}} = \sqrt{(\Delta R_{m,1}^{\text{TOA}})^2 + (\Delta R_{m,2}^{\text{TOA}})^2 + (\Delta R_{m,3}^{\text{TOA}})^2 + (\Delta R_{m,4}^{\text{TOA}})^2} \quad (10)$$

The relative uncertainty in TOA radiance due to four variables is computed as:

$$[(\Delta R_m^{\text{TOA}})/(R_m^{\text{TOA}})] \times 100. \quad (11)$$

Uncertainty due to surface reflectance anisotropy (BRDF effect)

Bidirectional reflectance distribution function is defined as the intrinsic property of a surface that describes the angular distribution of radiation reflected by the surface for all angles of exitance and under any given illumination geometry (Nicodemus *et al.*, 1977). In order to get the necessary data for the approximation of BRDF, a near-surface sensor instrument must be capable of acquiring reflectance data throughout the full range of hemispherical positions over a target. A goniometer is a device used to position a sensor at these different angles and azimuths.

The effect of surface reflectance anisotropy is not included in this study as the only product available was MODIS BRDF product at 500 m spatial resolution. The available MODIS product was generated based on the assumption that the surface is homogeneous in a pixel of 500 m, which is not the case here as we are dealing with the artificial target of few meters' size. The uncertainty due to Bidirectional Reflectance Factor is planned to include in the future work by using the ground measured values of the same using Goniometer.

4.2 Estimation of calibration constant using simple analytical approach

Suppose we have two artificial targets: one bright (say white cloth) and another dark (say black cloth). Their reflectances can be measured using ASD FieldSpec®3 Spectro-radiometer. It is a compact, field portable, and precision instrument with a spectral range of 350-2500 nm and a rapid data collection time of 0.1 second per spectrum. The SWIR component of the ASD spectrometer is a scanning spectrometer, while the VNIR component is an array spectrometer. If we assume that the bright and dark targets' reflectance's are ρ_1 and ρ_2 respectively. Using equation 1 we have,

$$L1(TOA)=a*DN1+b \quad (2)$$

$$L2(TOA)=a*DN2+b \quad (3)$$

where L1(TOA) and L2(TOA) are the radiance at the top of the atmosphere and DN1 and DN2 are the DN values in the image corresponding to bright and dark target respectively.

From equations (2) and (3), is easy to get

$$a = \frac{L_1(TOA) - L_2(TOA)}{DN_1 - DN_2} \quad (4.1)$$

$$b = L1(TOA) - ((L1(TOA) - L2(TOA)) / (DN1 - DN2)) * DN1 \quad (4.2)$$

It is easy to see that DN1 should be much greater than DN2, that is, their difference should be large. Otherwise, 'a' blows up. Since it is difficult to get white sand and water (for example) near to each other in real life, hence the need for artificial targets.

In order to simulate the TOA radiance, following equation is used:

$$L(TOA) = \frac{E_{sun} \times \cos(\theta) \times \rho^*}{\pi \times d^2} \quad (5)$$

where, d is the sun-earth distance in the Astronomical Units (AU), Esun is the bandpass exo-atmospheric solar irradiance for a particular spectral channel of a sensor and 'θ' is solar zenith angle, ρ* is apparent reflectance at the sensor level which can be calculated as:

$$\rho^* = \rho_a + \frac{\rho_t \times T_{\theta_v} \times T_{\theta_s}}{1 - \rho_t \times s} \quad (6)$$

where, ρ_a is the path radiance in terms of reflectance, 's' is spherical albedo of the atmosphere, T_{θ_v} & T_{θ_s} is the transmissivity of the atmosphere in the downward and upward direction respectively and ρ_t is the surface reflectance of the target.

Calibration constant is estimated using top-of-the-atmosphere radiance $L(\text{TOA})$ for each target (which in turn is estimated using equations 5 and 6) and corresponding DN values of the target from the satellite image using equations 4 & 5.

The main assumption that has been taken in the proposed methodology for the estimation of calibration constant with one date data and artificial targets is as follows:

- for the high resolution optical sensor Cartosat-2, the pixels are so close that the vertical structure of the atmosphere can be assumed to remain same for both the targets and hence the contribution of radiation due to scattering in the atmosphere without interaction with the surface is same for signal registered at sensor in the given band for both the pixels (bright and dark).

The path radiance term ρ_a is assumed to be constant for both the targets because of the above said assumption and hence it is cancelled out while estimating the calibration constant.

5. RESULTS AND DISCUSSION

The mean coefficient of variation corresponding to different targets for Cartosat-2 panchromatic band (450-850 nm) used in the study was found to be less than 3% (Figure 4). The maximum variability was found for black target and minimum corresponding to soil target.

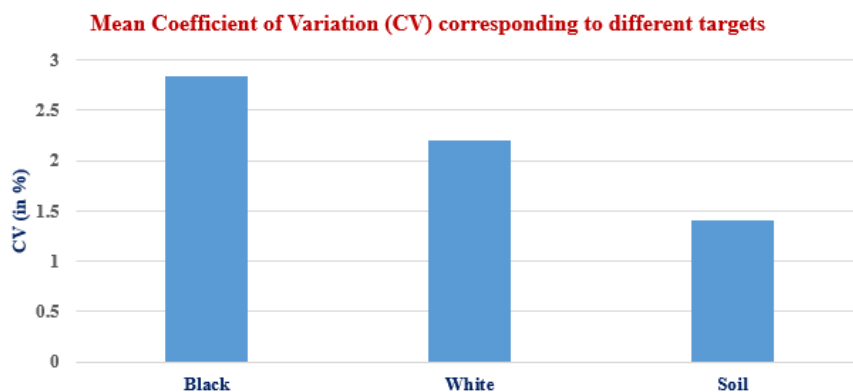


Figure 4: Mean Coefficient of variation

The reflectance of the targets was measured using ASD spectro-radiometer and its variation with wavelength is shown in Figure 5. The spectral variation over Cartosat-2 band is shown in Figure 6.

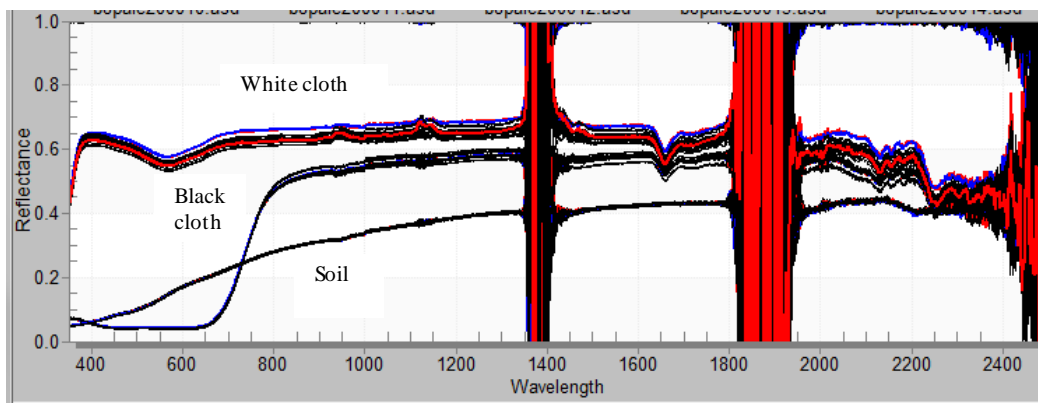


Figure 5: Variation of Reflectance of different targets with wavelength

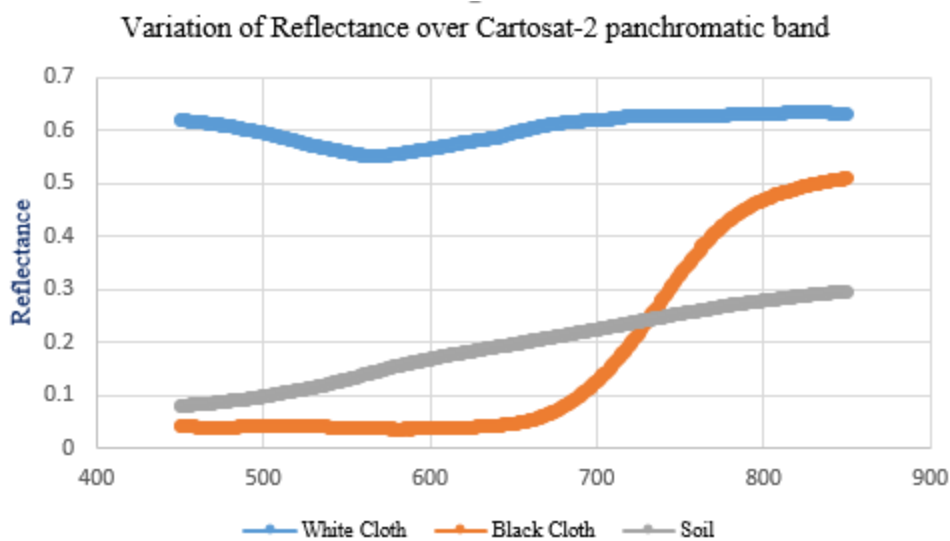


Figure 6: Variation of Reflectance of different targets over Cartosat-2 panchromatic band

It can be seen from Figure 6 that the reflectance of white cloth is more or less constant with wavelength and its mean value being 0.6 (approximately), whereas, the variation of black

cloth's reflectance is not constant over the entire bandwidth. Up till around 675 nm wavelength it remains constant with its value being (0.04) and after that it shoots up to 0.5. The variation in the reflectance of black cloth with wavelength indicates that this material is different than the white cloth material.

Artificial targets response on the Cartosat-2 image is shown in Figure 7. White cloth is captured well by the sensor as compared to the black cloth as can be seen from the image. This is due to the difference in the size and thickness of both the clothes. White cloth was bigger in size and thicker than the black cloth and the effect of which is evident in the response.



Figure 7: Response of artificial targets on Cartosat-2 image

5.1 Results using Vicarious calibration approach

Top-of-the-atmosphere radiances (L_{TOA}) were estimated using the approach mentioned in the methodology section. The 6S estimated and Cartosat-2 sensor observed TOA radiances using vicarious calibration for all the three targets are tabulated in Table 1.

Table-1: Estimated/Observed values of the parameters

Parameters	6S Estimated TOA radiance value (W/m²/sr/μm)	Cartosat-2 sensor observed TOA radiance value (W/m²/sr/μm)
L _{TOA} Black cloth	62.158	56.801
L _{TOA} Soil	77.458	68.138
L _{TOA} White cloth	208.607	136.8442

Table-2: Error analysis

Parameter	Target	TOA Radiance value for ±1σ change in parameter			Error+	Error-
		m	m+sd	m-sd		
AOD	<i>Black</i>	62.158	62.192	62.118	0.034	0.04
	<i>White</i>	208.607	208.153	209.14	-0.454	-0.533
	<i>Soil</i>	77.458	77.418	77.506	-0.04	-0.048
Ozone	<i>Black</i>	62.158	62.133	62.183	-0.025	-0.025
	<i>White</i>	208.607	208.463	208.751	-0.144	-0.144
	<i>Soil</i>	77.458	77.408	77.508	-0.05	-0.05
WV	<i>Black</i>	62.158	62.12	62.196	-0.038	-0.038
	<i>White</i>	208.607	208.516	208.699	-0.091	-0.092
	<i>Soil</i>	77.458	77.423	77.494	-0.035	-0.036
Radiance	<i>Black</i>	62.158	62.989	61.328	0.831	0.83
	<i>White</i>	208.607	213.238	203.992	4.631	4.615
	<i>Soil</i>	77.458	78.232	76.684	0.774	0.774

The uncertainty in mean value of TOA radiance value is calculated by perturbing each of the four independent variables (surface reflectance, Aerosol optical depth, ozone and water vapour) by $\pm 1\sigma$ from their mean values. The error due to individual four input variables is shown in Table 2 and total error is shown in Table 3.

Table-3: Uncertainty in mean value of TOA radiance estimated using vicarious approach

Target	Total Uncertainty -	Total uncertainty +	Relative Uncertainty (in%)
<i>Black</i>	0.833	0.832	1.34
<i>White</i>	4.656	4.649	2.23
<i>Soil</i>	0.777	0.778	1.00

Calibration coefficient calculated using mean value of TOA radiance estimated using vicarious calibration approach is shown in Figure 8. Multiplicative factor was found to be 0.475 ± 0.013 with additive factor being -46 ± 2.4 .

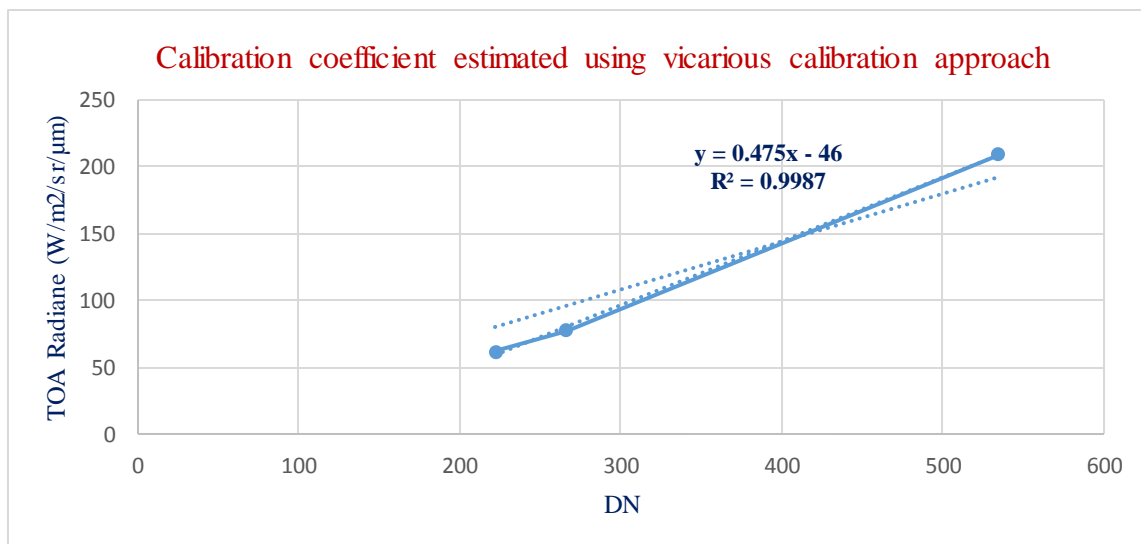


Figure 8: Estimated calibration coefficients using vicarious calibration approach

In order to the validation, estimated TOA radiance using vicarious approach was given as an input to 6S code and simulated surface reflectance was compared with the ground measured surface reflectance value. Results thus obtained are shown in table 5 and show that the surface reflectance estimated was found to be closer to the ground measured surface reflectance value (except for the black target) when TOA radiance estimated using vicarious calibration approach was used than the surface reflectance obtained using the Cartosat-2 sensor measured TOA radiance.

Table-5: Comparison of estimated surface reflectance with ground measured value

Target	Estimated surface reflectance		Ground measured surface reflectance (c)	Difference (in %)	
	Using Cartosat-2 sensor observed TOA radiance (a)	Using TOA radiance estimated using vicarious approach (b)		$\{(c-a)/c\} \times 100$	$\{(c-b)/c\} \times 100$
<i>Black</i>	0.1318	0.1504	0.1852	28.83	18.79
<i>White</i>	0.3828	0.6022	0.6009	36.29	0.22
<i>Soil</i>	0.1683	0.2007	0.2044	17.66	1.81

Further, in order to do the independent validation, the two radiance images were generated using the calibration constants estimated using this study and the calibration constants provided with the header file. The radiance of water body and the rooftop was compared and it was found that the radiance value of water body was found to decrease and of the rooftop was found to increase when the self-estimated calibration constant was used to generated the radiance image. It is planned in future to simulate the surface reflectance of the rooftop material at the SAC

main campus by using TOA radiance obtained using self-estimated calibration constants and 6S radiative transfer model and compare it with ground measured surface reflectance of the rooftop material for validation.

5.2 Results using simple analytical approach

Top-of-the-atmosphere radiances (L_{TOA}) were estimated using equations 5 and 6 and the mean value of the digital number corresponding to the target pixels were noted down from the satellite image. The estimated TOA radiances for all the three targets are tabulated in Table 6.

Table-6: Estimated/Observed values of the parameters

Parameters	Estimated/Observed Value
L_{TOA} Black cloth	78.214 (W/m ² /sr/μm)
L_{TOA} Soil	86.48 (W/m ² /sr/μm)
L_{TOA} White cloth	267.12 (W/m ² /sr/μm)
DN Black cloth	218
DN Soil	257
DN White Cloth	608

Table 1 shows that the TOA radiance for black cloth is almost similar to the TOA radiance of soil. The reason might be attributed to the fact that while installing the cloth, shoe markings must have left some soil on the cloth and while imaging, signature of soil could have been recorded. Because of this, the statistics calculated corresponding to the region of interest (ROI) extracted for black cloth might contain the signature of soil. The gain and offset i.e. multiplicative and additive factors were estimated using the correlation between DN values and TOA radiance. Figure 9 shows the graph between DN and TOA radiance.

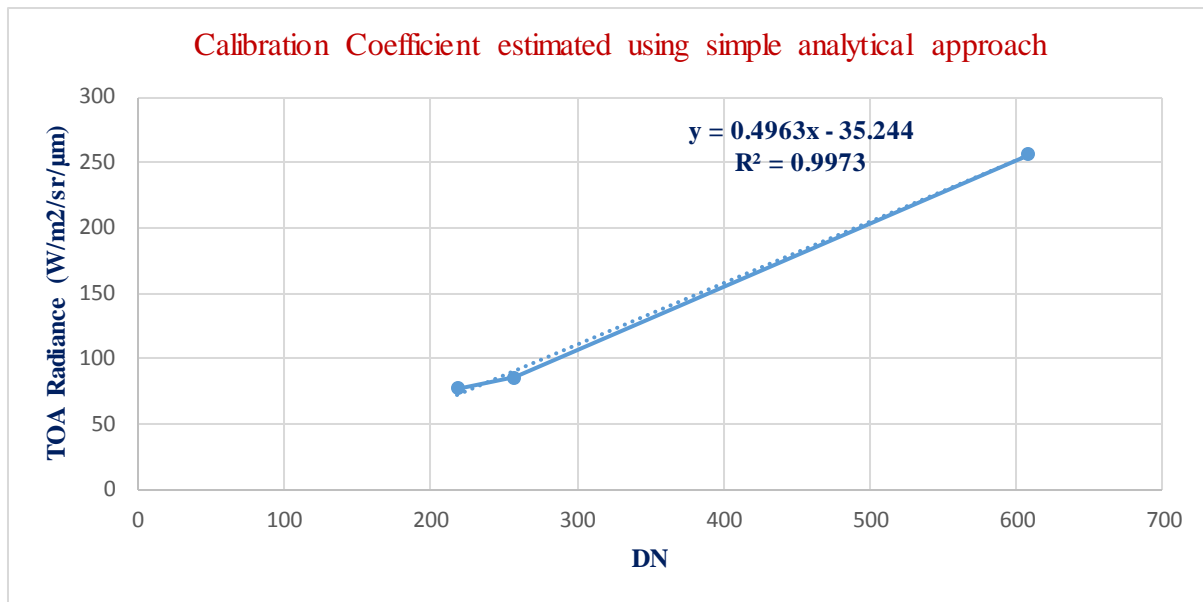


Figure 9: Estimated calibration coefficients using simple analytical approach

The comparison of the calibration constants estimated using vicarious approach and using simple analytic approach is shown in Table 7. It can be seen from the table that multiplicative and additive factor estimated using simple analytical approach is closer to the constants estimated using vicarious approach.

Table-7: Estimated calibration constants

Approach used	Estimated Multiplicative factor	Estimated Additive factor
Vicarious calibration approach	0.475±0.013	-46±2.4
Simple analytical approach	0.496±0.013	-35.24±1.62
Provided with header file	0.2557	0

6. CONCLUSIONS

In this study, the calibration constants for Cartosat-2 sensor were estimated using the image of 3rd may 2016 and artificial targets (black cloth and white cloth). Two independent approaches

were used for the estimation. One being the vicarious calibration, which is popularly used world-wide and other being physics based simple analytical approach. The multiplicative factor and additive factors were estimated using one date data only contrary to the method where large number of satellite image data is required for the estimation of calibration constant. The calibration activity indicates the change in the calibration constant for Cartosat-2 sensor. Both the vicarious and analytical approach show matching results with slight difference in the estimated mean value of multiplicative factors by vicarious and analytical approach. Although, more number of data is required for the refinement of the analytical model. The analytical approach will help in estimating the calibration factors for high resolution optical sensor viz. upcoming Cartosat-2C panchromatic and multispectral sensors using one date ground measurements only synchronous to satellite pass.

Acknowledgements

Authors gratefully acknowledge the encouragement and guidance received from Sri Tapan Misra, Director, Space Applications Centre, Ahmedabad. The support rendered by Dr. B. S. Gohil, Deputy Director, EPSA to carry out this activity is also thankfully acknowledged. Authors are grateful to Dr. Mehul Pandya for the technical discussions. Thanks are also due to Dr. Manish Saxena and Mrs. Deepa Padmanabhan for sharing the Cartosat-2 Relative response spectra. Authors thankfully acknowledge the cooperation and support provided by Mr. A. K. Singhal and Mr. R. N. Gouda for the maintenance of the SAC-Bopal calibration site. The help and support rendered by Mr. Mihir Rambhia, Mr. Vikram and Mr. Mayur during the field measurements were of utmost importance for the successful calibration campaign and authors express their sincere thanks to all of them.

References:

- [1] Datla et al., 2011) Best Practice Guidelines for Pre-Launch Characterization and Calibration of Instruments for Passive Optical Remote Sensing, R. U. Datla, J. P. Rice, K.Lykke and B. C. Johnson, NISTIR 7637 (Gregory, 2011, I. ARM handbook, DOE/SC-ARM/TR-056).
- [2] Dingirard, M., and P. N. Slater. 1999. "Calibration of Space Multi-Spectral Imaging Sensors: A Review." *Remote Sensing of Environment* 68: 194–205.
- [3] Vermote, E., D. Tanre, J. L. Deuze, M. Herman, J. J. Morcrette, and S. Y. Kotchenova. 2006. *Second Simulation of Satellite Signal in the Satellite Spectrum (6S). 6S User Guide Version 3*, University of Maryland.
- [4] V.N. Sridhar , Kaushal B. Mehta , R.P. Prajapati , K.N. Babu , N.M. Suthar & A.K.Shukla (2013): Absolute vicarious calibration of OCM2 and AWiFS sensors using a reflectance-based method over land sites in the Rann of Kutch, Gujarat, *International Journal of Remote Sensing*, 34:16, 5690-5708.